

Evolutionary constraints on the planet-hosting subgiant ϵ Reticulum from its white dwarf companion

J. Farihi,^{1*} M. R. Burleigh,¹ J. B. Holberg,² S. L. Casewell¹ and M. A. Barstow¹

¹Department of Physics & Astronomy, University of Leicester, Leicester LE1 7RH

²Lunar and Planetary Laboratory, University of Arizona, Tucson, AZ 85721-0063, USA

Accepted 2011 June 30. Received 2011 June 30; in original form 2011 April 5

ABSTRACT

The planet-hosting and Sirius-type binary system ϵ Reticulum is examined from the perspective of its more evolved white dwarf secondary. The stellar parameters are determined from a combination of Balmer line spectroscopy, gravitational redshift and solid angle. These three methods conspire to yield the most accurate physical description of the companion to date: $T_{\text{eff}} = 15\,310 \pm 350$ K and $M = 0.60 \pm 0.02 M_{\odot}$. Post-main-sequence mass-loss indicates that the current binary separation has increased by a factor of 1.6 from its primordial state when the current primary was forming its planet(s), implying $a_0 \geq 150$ au and constraining stable planets to within 15–20 au for a binary eccentricity of $e = 0.5$. Almost 80 years have passed since the first detection of the stellar companion, and marginal orbital motion may be apparent in the binary, suggesting a near edge-on configuration with $i \gtrsim 70^\circ$, albeit with substantial uncertainty. If correct, and all known bodies are coplanar, the mass of the planet HD 27442b is bound between 1.6 and 1.7 M_J .

A search for photospheric metals in the DA white dwarf yields no detections, and hence there is no clear signature of an extant planetary system orbiting the previously more massive secondary. However, if the white dwarf mass derived via spectral fitting is correct, its evolution could have been influenced by interactions with inner planets during the asymptotic giant branch. Based on the frequency of giant planets and circumstellar debris as a function of stellar mass, it is unlikely that the primordial primary would be void of planets, given at least one orbiting its less massive sibling.

Key words: binaries: general – stars: evolution – planetary systems – white dwarfs.

1 INTRODUCTION

Given that most stars form in binaries or multiples, understanding planet formation and evolution in the presence of two or more stars is fundamental. Furthermore, planets within binary star systems provide empirical constraints for formation theories and the dynamical models necessary to yield long-term, stable orbits (Heppenheimer 1974; Holman & Wiegert 1999).

ϵ Reticulum or HD 27442A is a K2 IV star with a gas giant planet in a 428 d orbit, whose minimum mass is 1.6 M_J (Butler et al. 2001, 2006), and a spatially resolved, faint stellar companion first detected nearly 80 years ago and found to be in the same relative position three and a half decades later (Mason et al. 2001). The common proper motion of HD 27442B was established by Raghavan et al. (2006), recognizing it as a stellar companion to a planet-host star. The nature of the secondary star was first constrained by Chauvin et al. (2006), finding that only a white dwarf was consis-

tent with the optical and near-infrared photometry at the 18.2 pc trigonometric parallax distance to the primary. The hydrogen-rich, degenerate nature of HD 27442B was confirmed via optical spectroscopy that revealed the distinct, pressure-broadened H α absorption profile typical of DA white dwarfs (Mugrauer, Neuhäuser & Mazeh 2007). Hence this system is a nearby Sirius-type binary hosting at least one planet.

The white dwarf is not yet listed in the catalogue of McCook & Sion (2008, 1999), nor in the 20 pc sample of Holberg et al. (2008), but should be designated WD 0415–594 based on its B1950 coordinates, as is convention. However, it is discussed in Holberg (2009) and Sion et al. (2009), both of which consider the fraction of white dwarfs present in binary systems. HD 27442 is among the 11 known Sirius-type systems within 20 pc and is one of three within this distance known also to harbour planets; the others being GJ 86 and HD 147513 (Desidera & Barbieri 2007).

Combined with the compact stellar radius implied by the distance to the primary, the spectrum obtained by Mugrauer et al. (2007) clearly establishes the secondary as a white dwarf. However, the shape and strength of H α are relatively degenerate over a broad

*E-mail: jf123@star.le.ac.uk

range of T_{eff} and $\log g$, while spectroscopy of the higher Balmer lines can effectively separate and uniquely determine these two parameters. (Bergeron, Saffer & Liebert 1992). This paper presents a determination of T_{eff} and $\log g$ for HD 27442B via high-resolution optical–ultraviolet spectroscopy of the entire detected Balmer series up to $H\beta$. This new and accurate information is harnessed and combined with reliable system parameters to place limits on the stellar masses and binary separation during the epoch of planet formation and to trace out the likely post-main-sequence dynamical history.

2 OBSERVATIONS AND DATA

2.1 UVES echelle spectroscopy

HD 27442B was observed on 2008 October 20 at Cerro Paranal with the 8.2-m Very Large Telescope using the Ultraviolet and Visual Echelle Spectrograph (UVES; Dekker et al. 2000) on Unit Telescope 2. Echelle spectroscopy was performed over the two detectors covering wavelengths 3200–6650 Å using a standard dichroic configuration with central wavelengths $\lambda_c = 3900/5640$ Å, resulting in two narrow gaps in spectral coverage near 4550 and 5650 Å. A single exposure of 1800 s was obtained using a slit width of 0.5 arcsec with 1×1 binning, resulting in a nominal resolving power of $R \approx 80\,000$ in both the UV-Blue and Red arms of the instrument. The featureless white dwarf WD 0000–345 (also LHS 1008) was observed for programme 382.D–0804(A) as a spectral standard on 2008 October 8 using an identical UVES setup but with 2×2 binning.

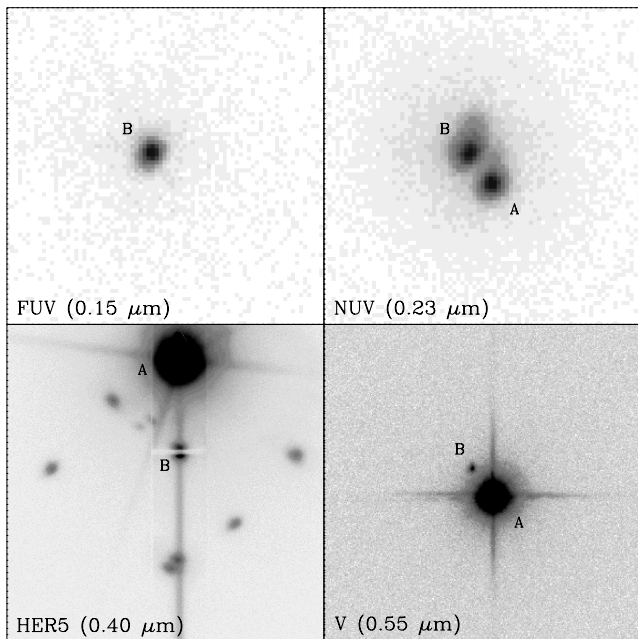


Figure 1. Upper panels: *GALEX* far- and near-ultraviolet images of HD 27442AB. In the epoch 2007.77 near-ultraviolet frame the pair appear separated by 14.0 arcsec at position angle $35^\circ 1$. Lower right: CTIO 0.9 m V-band CCD image of HD 27442AB in a 1 s exposure. These three frames are all north up, east left and approximately 2 arcmin on a side. Lower left: UVES acquisition frame of the science target in the slit, taken through a below-slit filter with central wavelength near 0.40 μm . The acquisition image is roughly 45 arcsec square and oriented along the binary axis, at approximately 235° . The CCD bleed from the saturated primary does not correspond to stray light entering the slit.

Fig. 1 reveals that no difficulty was encountered obtaining the secondary spectrum in the presence of its much brighter primary; neither the extended stellar image halo nor the telescope support diffraction spikes fall across the slit. Therefore, the spectrum of HD 27442B is uncontaminated by the light of the bright primary. However, in addition to the fact that science target and standard star were observed on separate nights, there was also a significant difference in airmass between these observations, $\Delta \sec z \approx 0.45$. Hence, the overall shape of the reduced spectrum is potentially skewed by differential extinction, owing to both night-to-night and airmass variations between science and standard targets, especially at the shortest wavelengths.

The echelle data were processed with the UVES pipeline version 4.3.0 using *GASGANO*, including cosmic ray masking, flat fielding, wavelength calibration, order merging, and distilled using optimal aperture extraction. The science target data were then interpolated in wavelength to match the solution for the spectral standard, divided by the standard spectrum, and multiplied by an appropriate temperature blackbody for relative flux calibration. It was found at this stage that the three spectral orders did not match at their adjacent ends, and corrective factors were applied to these residual offsets prior to re-normalization. The fully reduced spectrum still contains ripples that are often associated with UVES data, but which could not be removed in this high signal-to-noise ratio (S/N) data set; the quality control parameter *rplpar*, which should be much less than 5 according to the UVES manual, was less than 0.6 for all extracted orders. The normalized spectrum of HD 27442B is displayed in Fig. 2.

2.2 Supplementary data

Perhaps unsurprisingly, there is a spatially well-resolved detection of the white dwarf companion in *Galaxy Evolution Explorer* (*GALEX*; Martin et al. 2005) images of HD 27442, shown in Fig. 1. In fact, the white dwarf outshines the K2 subgiant star in the near-ultraviolet at 2300 Å, and is the only emission source seen in the far-ultraviolet at 1500 Å. Roughly speaking, the binary offset apparent in the *GALEX* image is similar to those determined by Chauvin et al. (2006) and Mugrauer et al. (2007), as well those given in the Washington Double Star Catalog (Mason et al. 2001) based on observations made 45 and 80 years prior.

As of this writing, the SIMBAD IRCS coordinates for HD 27442B are essentially no different from that of the primary. Taking a nominal offset from this position and extrapolating back to epoch 2000.0 using the well-measured proper motion of the system gives a J2000 position for the white dwarf of $04^{\text{h}}16^{\text{m}}30^{\text{s}}.0$, $-59^\circ 17' 58''$ (and a B1950 position of $04^{\text{h}}15^{\text{m}}37^{\text{s}}.7$, $-59^\circ 25' 17''$, hence WD 0415–594).

There is a corresponding faint *ROSAT* source centred 18 arcsec from the J2000 position of the primary (1RXS J041631.2–591815; Voges et al. 2000). The X-ray detection has an 18 arcsec position error, and hence could be associated with either binary component. Furthermore, the hardness ratio indicates that the source is only emitting in the 0.1–0.4 keV band, but only white dwarfs hotter than 25 000 K are significant sources of soft X-rays (O’Dwyer et al. 2003). Observations taken with the *International Ultraviolet Explorer* (*IUE*; Boggess et al. 1978) of HD 27442A reveal emission features over the 1000–2000 Å region, notably very strong Lyman α . Therefore, it is likely that coronal emission from the cool primary is the source of the detected X-rays (i.e. flaring).

Table 1 lists available ultraviolet, optical and near-infrared photometry for the two stellar binary components. The only available

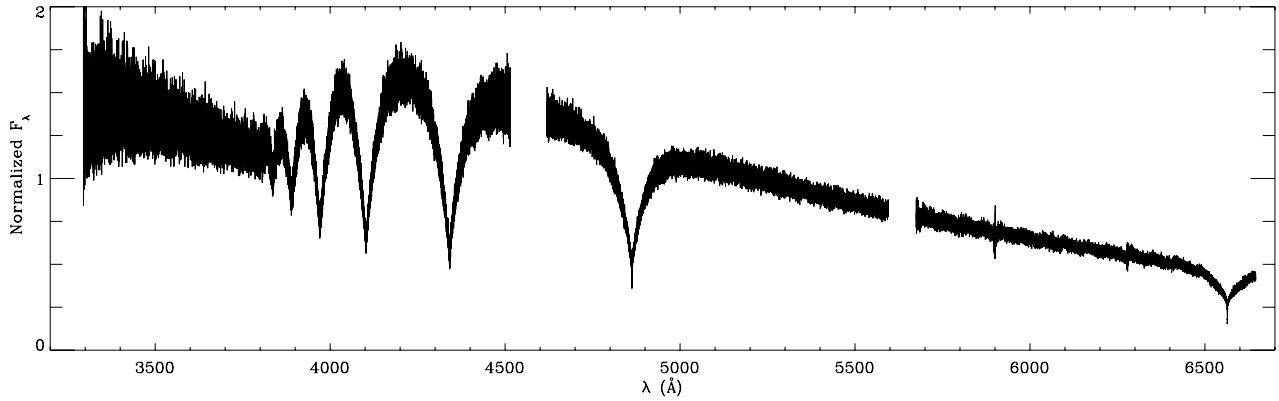


Figure 2. UVES spectrum of the white dwarf HD 27442B. The science target data were interpolated and rebinned in the spectral direction to match the wavelength solution of the DC white dwarf observed for sensitivity and flux calibration purposes, but the data are otherwise unsmoothed. The features near 5900 and 6300 Å are detector artefact and telluric absorption residuals, respectively. The quasi-periodic pattern in the spectrum is due to a light-path difference between the flat-field lamp and the sky; this interference is not fully correctable, especially at high S/N.

Table 1. Observed and derived properties of HD 27442.

Component	B	A
Photometry:		
FUV (AB mag)	12.7	–
NUV (AB mag)	12.6	13.0
<i>U</i> (mag)	–	6.6
<i>V</i> (mag)	12.5	4.4
<i>I</i> (mag)	–	3.4
<i>H</i> (mag)	12.9	2.1
Astrometry:		
d_{π} (pc)	–	18.2
v_{rad} (km s ^{−1})	–	+28.7
(μ_{α} , μ_{δ}) (mas yr ^{−1})	–	(−48.0, −167.8)
(<i>U</i> , <i>V</i> , <i>W</i>) (km s ^{−1})	–	(−25, −17, −12)
Parameters:		
SpT	DA3.3	K2 IV
T_{eff} (K)	15 310 ± 350	4850
log <i>g</i> (cm s ^{−2})	7.98 ± 0.02	3.78
<i>M</i> (M _⊙)	0.60 ± 0.02	1.54
M_{ms} (M _⊙)	1.9	–
Cooling age (Gyr)	0.2	–
MS age (Gyr)	1.3	–
Total age (Gyr)	1.5	2.8

Note. The white dwarf mass and cooling age are based on the models of Fontaine, Brassard & Bergeron (2001), with a main-sequence lifetime estimated using the formulae of Hurley, Pols & Tout (2002). Remaining table entries are based on various catalogues and literature sources (Bessell 1990; Perryman et al. 1997; Mason et al. 2001; Martin et al. 2005; Butler et al. 2006; Mugrauer et al. 2007; Takeda et al. 2007). The 2MASS data for the bright primary are heavily saturated; Gezari, Pitts & Schmitz (1999) give $J = 2.57$ mag and $K = 1.97$ mag, consistent with the adopted *H*-band magnitude.

near-infrared *JK* photometry of HD 27442B has substantial uncertainty (Chauvin et al. 2006), as it is based on the highly saturated Two Micron All Sky Survey (2MASS) photometry for HD 27442A. However, the secondary *H*-band photometry of Mugrauer et al. (2007) was derived using non-adaptive optics images and standard photometric calibration with multiple 2MASS sources in the image field (M. Mugrauer, private communication), and should therefore be reliable.

3 ANALYSIS

3.1 White dwarf parameter determination

3.1.1 Balmer spectroscopy

The spectrum of the white dwarf was fitted using a grid of (LTE) pure hydrogen atmosphere models as described in Koester (2010). Comparison between the models and the UVES data was performed using the spectral-fitting routine FITSB2, as described in some detail in Casewell et al. (2009). Results of the spectral analysis yield $T_{\text{eff}} = 15310 \pm 20$ K and $\log g = 7.88 \pm 0.01$, including only the formal errors of the Balmer line fitting procedure.

There is a significant body of literature on the effective temperatures and surface gravities of hydrogen-rich white dwarfs as derived via Balmer line spectroscopy (Bergeron, Saffer & Liebert 1992; Bergeron, Liebert & Fulbright 1995). Recently, two studies have obtained multiple spectra for each of hundreds of DA stars, permitting an assessment of errors beyond those derived from the spectral-fitting procedure (which are merely a function of S/N): one using single-order, low-resolution data (Liebert, Bergeron & Holberg 2005) and the other with high-resolution, echelle spectroscopy (Koester et al. 2009). Typical standard deviations in these studies are found to be 1.2 and 2.3 per cent in T_{eff} , 0.04 and 0.08 dex in $\log g$, with the higher variance observed in echelle data, its intrinsic complexity the likely culprit (Koester et al. 2009).

Particularly appropriate are the results of the SPY survey (Napiwotzki et al. 2003), which observed hundreds of DA white dwarfs with UVES using an instrumental configuration and calibration procedure identical to that adopted for HD 27442B. Koester et al. (2009) report a systematic offset of -0.08 dex in $\log g$ and $+1.2$ per cent in T_{eff} for 85 single, and well-behaved DA white dwarfs in common with Liebert et al. (2005). Despite the high S/N spectrum of HD 27442B, the aforementioned results imply realistic parameters of $T_{\text{eff}} = 15310 \pm 350$ K, $\log g = 7.88 \pm 0.08$, with the possibility that the surface gravity and mass have been systematically underestimated.

3.1.2 Gravitational redshift

The apparent velocity of the secondary was determined using both Gaussian and Lorentzian fits to the relatively sharp, non-LTE cores of $H\alpha$ and $H\beta$, yielding $+58.0 \pm 0.5$ km s^{−1}, including

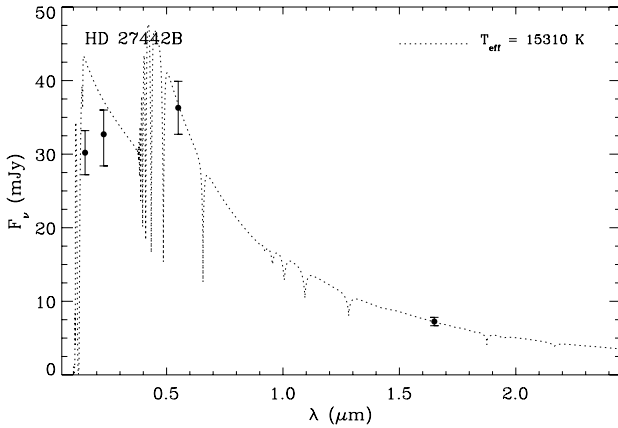


Figure 3. Spectral energy distribution of HD 27442B. The model effective temperature broadly matches the optical through near-infrared colour, though the *GALEX* ultraviolet photometry is somewhat discrepant.

an instrumental stability uncertainty of 0.4 km s^{-1} (R. Napiwotzki, private communication). This observed velocity is the sum of four components:

$$v_{\text{app}} = \gamma + v_{\text{orb}} + v_{\text{grav}} + v_{\text{bary}}. \quad (1)$$

The systemic velocity (γ) is subsumed by the total radial velocity ($\gamma + v_{\text{orb}}$) of the primary star, for which there are at least four similar measurements published between 1913 and 1928, with $+29.3 \pm 0.5 \text{ km s}^{-1}$ listed in the General Catalogue of Stellar Radial Velocities (Wilson 1953). Much more recently, one of the precision radial velocity monitoring campaigns has measured $+28.7 \pm 1.6 \text{ km s}^{-1}$ (the quoted error is overconservative as the instrumental stability is better than 0.3 km s^{-1} ; Jenkins et al. 2011). The barycentric velocity towards the science target on the UVES observation date was -1.0 km s^{-1} .

From the current projected separation of the pair, the maximum orbital speed is 2.8 km s^{-1} , while averaging over $\sin i$ for the unknown orbital inclination predicts that the observed velocity should be within $\pm 1.8 \text{ km s}^{-1}$. This latter value is adopted as the $2\sigma_{\text{orb}}$ error, with $3\sigma_{\text{orb}} = 2.7 \text{ km s}^{-1}$ corresponding to the worst case scenario. Thus, adding in quadrature the 1σ uncertainties in the measured apparent velocity (0.5 km s^{-1}), measured radial velocity (1.6 km s^{-1}) and orbital velocity (0.9 km s^{-1}) of the system yields $v_{\text{grav}} = +30.3 \pm 1.9 \text{ km s}^{-1}$. This value suggests a higher mass for the white dwarf than predicted by the model fit to the Balmer lines.

3.1.3 Solid angle

A third, largely independent check of the white dwarf radius can be made because the system has a precise parallax measurement of $\pi = 54.83 \pm 0.15 \text{ mas}$ (van Leeuwen 2007). The solid angle subtended by the star in the sky, and thus $(R/D)^2$, can be determined by fitting a flux-calibrated spectral model to the observed stellar flux at the Earth. Fig. 3 displays the best fit of the spectroscopically derived model to the data, weighted heavily towards the observed $H = 12.871 \pm 0.085 \text{ mag}$ (Mugrauer et al. 2007), as it is the only published (non-adaptive optics) photometric datum with a reliable error. From the fitting process, a range of acceptable fits are found for $R = 0.01320 \pm 0.00045 R_{\odot}$.

Table 2. Mass–radius determinations for HD 27442B.

Method	Radius (R_{\odot})	Mass (M_{\odot})
Balmer spectroscopy	0.0141 ± 0.0006	0.547 ± 0.043
Gravitational redshift	0.0129 ± 0.0003	0.616 ± 0.022
Solid angle	0.0132 ± 0.0005	0.599 ± 0.027
Weighted average	0.0132 ± 0.0002	0.602 ± 0.016
χ^2 minimization	0.0133 ± 0.0007	0.616 ± 0.068

Note. For $M_{\text{B}} \lesssim 0.58 M_{\odot}$, the predicted main-sequence progenitor mass is lower than the mass of the less evolved primary.

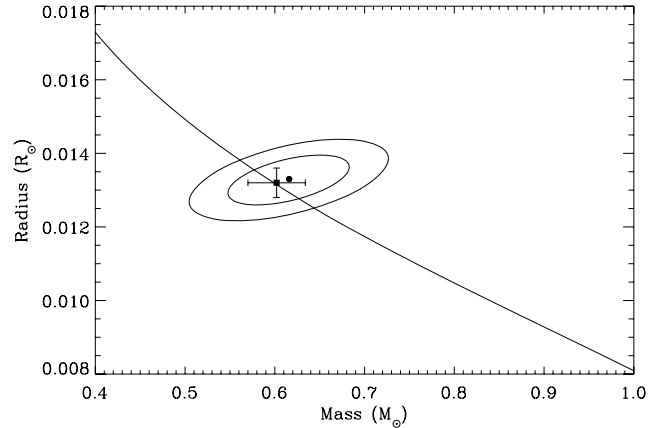


Figure 4. Theoretical mass–radius relation for a 15310 K DA white dwarf (diagonal curve) plotted with the semi-empirical constraints derived for the photometric radius, surface gravity and gravitational redshift measurements discussed in Section 3.1. The resulting minimum $\chi^2 = 1.65$ is indicated by a filled circle along with 1 and 2σ contours. For comparison, the weighted average mass and radius are plotted as a square with 2σ error bars.

3.1.4 Adopted values and evolutionary considerations

For many white dwarfs where T_{eff} and $\log g$ are determined spectroscopically, a mass is routinely calculated based on an assumed, theoretical mass–radius relation. In the case of HD 27442B, however, there are two additional observations that can be used to determine masses and radii: the photometric solid angle (and parallax) and the gravitational redshift. Because the solid angle constrains only R , the surface gravity only M/R^2 and the gravitational redshift only M/R , it is necessary to use a mass–radius relation to determine both parameters. Each separate constraint can be used with a mass–radius relation to make independent estimates of mass and radius and associated uncertainties. These independent results need not agree precisely but ought to be reasonably consistent. Table 2 lists the results for the three observational constraints on the stellar mass and radius. Fig. 4 plots the mass–radius relation¹ (Holberg & Bergeron 2006; Fontaine et al. 2001) adopted here.

The mass and radius of HD 27442B derived via gravitational redshift and solid angle agree rather well, predicting a mass roughly 10 per cent higher than the spectroscopic method. A higher white dwarf mass is superior when viewed in the context of the binary history. A current mass of $0.60 M_{\odot}$ corresponds to a progenitor mass near $1.9 M_{\odot}$ (Kalirai et al. 2008), while the spectroscopically derived value of $0.55 M_{\odot}$ implies a progenitor that was (likely, but

¹ <http://www.astro.umontreal.ca/~bergeron/CoolingModels>

not certainly) less massive than HD 27442A ($1.6 M_{\odot}$; Takeda et al. 2007). Given the close agreement between the stellar parameters derived via redshift and solid angle, and the possible paradox implied by the lower mass derived via spectroscopy, it is tempting to favour higher mass values. Furthermore, the finding of Koester et al. (2009) that Balmer line fitting in UVES spectra may underestimate the white dwarf surface gravity makes the lower mass suspect.

If the mass derived via the Balmer line fitting is correct, some process has reduced the white dwarf mass to a value 10 per cent lower than expected via single star evolution. In this case, a main-sequence star of $M > 1.6 M_{\odot}$ would have descended into a $0.55 M_{\odot}$ remnant. Since the binary has always been sufficiently wide as to preclude mass transfer, this potential conundrum cannot be resolved via an Algol-type history. One possibility is enhanced mass-loss along the first ascent giant branch, during the growth of the degenerate core mass, due to the interactions with one or more inner, giant planets (Siess & Livio 1999a,b). While speculative, it is consistent with the presence of a planetary system within the binary and reasonable expectations for planet formation at intermediate-mass stars (Johnson et al. 2007; Lovis & Mayor 2007; Bowler et al. 2010).

Another model-independent way of considering the various possible solutions to the radius and mass associated with observed photometry, surface gravity and gravitational redshift of HD 27442B is to treat all of these as independent constraints on the stellar radius as a function of mass. Under this type of analysis the radius and mass are determined without explicit reference to any mass–radius relation and the most likely mass and radius with associated uncertainties are determined from a minimum χ^2 calculation. How these joint constraints are related to the appropriate mass–radius relation is shown in Fig. 4. From this method the minimum χ^2 corresponds to a mass and radius of $0.616 M_{\odot}$ and $0.0133 R_{\odot}$, respectively. While this result is consistent with the expected mass–radius relationship and the weighted average of the results in Table 2, it yields a somewhat higher mass compared to the weighted average of $0.602 M_{\odot}$. This is primarily driven by the fact that the mass–radius-based determinations will lie closer to the mass–radius relation from which they are derived. In summary, both the mass–radius-based determinations and the minimum χ^2 calculation give consistent results, where the χ^2 1σ contour encloses the mass–radius relation for masses between 0.577 and $0.628 M_{\odot}$.

3.2 Evidence of two planetary systems?

Because the main-sequence progenitor of the extant white dwarf secondary was more massive than the current planet-bearing primary, it is logical that a substantial protoplanetary disc would have orbited HD 27442B. Hence it is possible that planets would have formed first, and perhaps more readily, at HD 27442B, corroborated by studies that show that giant planets and signatures of planetary systems are found more often at higher mass stars (Su et al. 2006; Trilling et al. 2008; Bowler et al. 2010). Currently, any putative planets orbiting beyond 50 au at either stellar component are unstable; yet each star may retain planets within a few tens of au if the binary orbital eccentricity is mild. While planetary system remnants orbiting white dwarfs are likely to be found outside 5 au (Burleigh, Clarke & Hodgkin 2002; Nordhaus et al. 2010), hence leaving a relatively narrow region in which such objects may persist at HD 27442B, their signatures are sometimes found via heavy element pollution in an otherwise pure hydrogen or helium atmosphere (Farihi et al. 2010; Zuckerman et al. 2010).

The spectrum of HD 27442B was examined by eye for photospheric metal lines observed in DAZ white dwarfs of similar

effective temperature; calcium K absorption being by far the most prominent for a typical polluted white dwarf (Zuckerman et al. 2003). Despite the excellent data quality, the search was unsuccessful. The S/N was estimated to be around 80 in a 300 pixel, 4 Å interval around the calcium K-line (3933.7 Å). This estimate comes from the raw, unbinned, extracted spectrum and uncorrected for the highly curved shape in this region, and hence the true S/N is certain to be higher. Based on comparable but lower S/N UVES observations of similar DA white dwarfs with and without metals, a calcium abundance of $\log [n(\text{Ca})/n(\text{H})] > -9.0$ can be firmly ruled out (Koester et al. 2005).

3.3 Spectral energy distribution

Fig. 3 plots the *GALEX*, *V*- and *H*-band photometry for HD 27442B (Mason et al. 2001; Martin et al. 2005; Mugrauer et al. 2007), together with the spectral model fitted to the UVES data. The *GALEX* data are uncorrected for extinction, which should be mild at a distance of 18 pc, and the single measurements for each component and each bandpass were assigned 10 per cent errors based on this uncertainty (the quoted errors are less than 1 per cent, which is unrealistic). It is not clear from the *GALEX* catalogue documentation whether the photometry of either component is problematic (e.g. too bright) or contaminated by its companion; hence, the error assignment is also based on this additional uncertainty. As can be seen in Fig. 3, the ultraviolet flux of the optically derived model disagrees somewhat with the *GALEX* photometry, even with the greatly augmented error bars. Possible reasons for this are beyond the scope of the current work.

3.4 Evidence for orbital motion?

Astrometric observations of HD 27442AB exist as early as 1930 and 1964 (Mason et al. 2001). Table 3 lists those data together with relatively recent, near-infrared adaptive optics astrometry for the pair. Although the primary star is badly saturated in the 1 s exposure of the *V*-band image obtained at CTIO (Fig. 1), two methods were used to obtain a centroid. First, the diffraction spikes resulting from the secondary mirror supports were fitted with lines whose intersection should coincide with the astrometric centre of the star. Secondly, a weighted centroid was measured for hundreds of linear pixels after removal of non-linear and saturated data. Both of these methods produced agreeable results for the primary star, to within a single pixel, and the average offset resulting from those values is listed in Table 3.

Table 3. Astrometric observation summary for HD 27442AB.

Epoch (yr)	Separation (arcsec)	PA (deg)	Reference
1930.1 ^a	13.68	33.9	Jessup (1955)
1964.9 ^a	13.82	36.3	Holden (1966)
2003.7 ^b	12.94 ± 0.08	36.7 ± 0.4	Mugrauer et al. (2007)
2004.7 ^c	13.07 ± 0.02	36.4 ± 0.2	Chauvin et al. (2006)
2004.8	12.8 ± 0.2	36.3 ± 0.9	CTIO <i>V</i> -band
2007.8	14.0 ± 0.2	35.0 ± 0.8	<i>GALEX</i> NUV

^aThe details of the earliest observations were provided by B. Mason (private communication) and do not have error determinations.

^bAverage epoch and offsets for two observations.

^cAverage epoch and offsets for three observations.

The *GALEX* near-ultraviolet pipeline frame has by far the lowest contrast between components among any available image of the binary, and computing reliable centroids from this image was straightforward. However, the measured separation in that image (Table 3) disagrees significantly with three other recent measurements, whose mean is 12.93 ± 0.14 arcsec at a mean epoch of 2004.4. The *GALEX* pixel scale is large at 1.5 arcsec, and while Morrissey et al. (2007) report a 1σ error of 0.5 arcsec in *absolute* position for bright point sources within the central 0.6 of the near-ultraviolet image fields (which applies to HD 27442), this should not affect the *relative* astrometry for two nearby point sources. Given this notable deviation from the other measures, the *GALEX* offsets may not be accurate.

The 1930 and 1965 observations give an average projected separation near 250 au and thus $P \geq 2665$ yr for a total binary mass of $2.2 M_{\odot}$. A face-on orbit is unlikely given (1) the radial velocity-detected planet at the primary (assuming planet–binary coplanarity as the most probable configuration) and (2) an expected $\dot{\theta} = 0.090\text{--}0.135 \text{ yr}^{-1}$ orbital motion for $e = 0\text{--}0.5$ or $3.6\text{--}5.4$ over 40 yr that has not been observed. Thus, it is likely the binary has $i \gtrsim 70^{\circ}$. A circular, edge-on orbit is consistent with a 0.8 arcsec change in separation (if real) between 1964 and 2004. For this case, one gets $a = 385$ au and $P = 5090$ yr by numerically solving orbital equations and Kepler’s third law simultaneously, suggesting that the 2004 projected separation would be around $0.6a$. Without precise and accurate astrometry over decade time-scales, further constraints on the binary orbit are unlikely to be forthcoming.

While the wide binary orbit is largely unconstrained, these rough estimates indicate that highly inclined orbits are unlikely (consistent with the radial velocity-detected planet), while orbits edge-on yield likely semimajor axes a bit larger than 1.6 times the current projected separation.

3.5 Planet formation in the former A/F star binary

Table 1 lists the resulting main-sequence parameter constraints for HD 27442B based on current mass estimates of the primary star. In this case, there is poor agreement between the age estimate of HD 27442A and the predicted main-sequence lifetime plus cooling age of its companion. Both the initial-to-final mass relation (Williams, Bolte & Koester 2009) and main-sequence lifetimes (Hurley et al. 2002) are steep functions as stellar mass decreases below $1.6 M_{\odot}$, and thus if the mass of the primary is a few per cent lower than the adopted value, the potential for better agreement between the total ages of the components grows rapidly. If the adopted white dwarf and progenitor masses for HD 27442B are essentially correct, then its main-sequence lifetime is only 1.3 Gyr and the total system age is under 1.5 Gyr.

With both stars on the main sequence, the semimajor axis of the binary was shorter by a factor of (Jeans 1924)

$$\frac{a_0}{a} = \frac{M_B + M_A}{M_{\text{ms}} + M_A}. \quad (2)$$

This ratio is not very sensitive to the spread in possible values for each mass and gives an average value of $a_0 = 0.62a$ for the various possibilities based on this work and the published mass estimates of the primary (Butler et al. 2006; Takeda et al. 2007). If the current projected separation reflects the current semimajor axis, then $a_0 \approx 150$ au. Fig. 5 plots the resulting orbital constraints when the pair were both on the main sequence, for both the stellar and planetary companions. The critical radius for planet stability

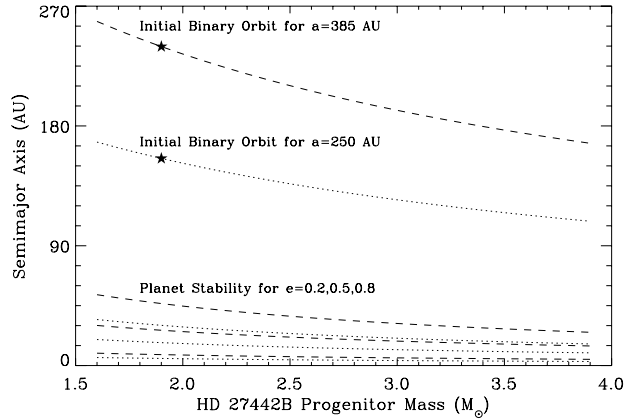


Figure 5. Possible semimajor axes for HD 27442AB during the epoch of planet formation, plotted as a function of the progenitor mass of the white dwarf secondary. The star symbol denotes the value resulting from the adopted white dwarf mass in Table 1. Also shown is the critical semimajor axis beyond which planetary orbits are unstable; this depends strongly on the binary eccentricity which is unknown but likely to be substantial given $P > 10^3$ yr (Section 3.5).

(Holman & Wiegert 1999) shown in the figure corresponds to the a_0 derived here.

As a pair of main-sequence stars near 1.5 and $1.9 M_{\odot}$, the likely spectral types of HD 27442B and A should be around A5 and F0, respectively (Drilling & Landolt 2000). For their initially wide binary orbit, strong constraints on planetary orbit stability arise only for significant binary eccentricities. For the intermediate-mass stars in question with an initial period of $P > 10^3$ yr, a mean eccentricity of 0.5 is expected (Abt 2005), and therefore planetary orbit stability would have been confined to within 15–20 au.

3.6 Total age

Using the stellar evolutionary formulae of Hurley et al. (2002), a main-sequence lifetime of 2.3–2.8 Gyr results for a star with a mass in the range $1.49\text{--}1.59 M_{\odot}$ as estimated for HD 27442A (Butler et al. 2006; Takeda et al. 2007). Given that the primary in this system has recently left the main sequence, and that the subsequent evolutionary phases are much shorter lived than the hydrogen burning lifetime, the above is a good estimate for the total lifetime of the binary and planet-host system. However, for main-sequence masses near $1.9 M_{\odot}$, the total age of the white dwarf should be less than 1.5 Gyr. If the 2.8 Gyr age estimate of Takeda et al. (2007) is accurate, this would argue for a longer progenitor lifetime for HD 27442B and in the direction of the lower white dwarf mass as derived from spectroscopy.

4 CONCLUSIONS

The optical spectrum of the white dwarf companion to the planet-hosting star HD 27442A yields a reliable effective temperature, and three, mostly independent, determinations of its radius and mass. These results combine to support a picture whereby planets orbiting HD 27442A within tens of au have always been stable, but indicate a total system age that is significantly younger than previous estimates. The white dwarf HD 27442B does not exhibit photospheric metals indicative of a remnant planetary system, but its more massive progenitor was capable of hosting stable planets within tens of au.

Assuming the star–star and star–planet planes are all co-aligned leads to likely binary orbits near edge-on, but substantial uncertainty remains. If orbital motion is apparent in the past 40 yr, the semi-major axis is larger than the current projected separation, leading to current periods up to 5100 yr. On the other hand, if the projected separation reflects the semimajor axis, the period is closer to 2500 yr. From these estimates, it is found that the binary system was no closer than 150 au at the time of planet formation, and only a high eccentricity should have affected stable planetary orbits within 20 au at HD 27442A.

Future, precision astrometric measurements should be able to confirm or rule out orbital motion on decade time-scales, while ongoing studies of the exoplanet can similarly identify any trend in the radial velocity of the primary at the 10 m s^{-1} level. Such observations would place the best possible constraints on the binary semimajor axis. Optical and near-infrared photometry at the few per cent level would better constrain the effective temperature and radius of the white dwarf, providing a more precise estimate of the binary separation during the epoch of planet formation.

ACKNOWLEDGMENTS

JF thanks T. Henry and D. Raghavan for sharing their optical images of HD 27442. The authors thank the referee G. Chauvin for comments which improved the quality and clarity of the manuscript. D. Koester kindly provided his atmospheric models of the white dwarf for spectral fitting. [Balmer lines in the models were calculated with the modified Stark broadening profiles of Tremblay & Bergeron (2009) kindly made available by the authors.] JF acknowledges the support of the STFC. JBH wishes to acknowledge support from NSF grant AST-1008845. Based on observations made with ESO Telescopes at Paranal Observatory under programme 382.D-0186(A). This work includes data taken with the NASA *Galaxy Evolution Explorer*, operated for NASA by the California Institute of Technology under NASA contract NAS5-98034.

REFERENCES

Abt H. A., 2005, *ApJ*, 629, 507
 Bergeron P., Saffer R. A., Liebert J., 1992, *ApJ*, 394, 228
 Bergeron P., Liebert J., Fulbright M. S., 1995, *ApJ*, 444, 810
 Bessell M. S., 1990, *A&A*, 83, 357
 Boggess A. et al., 1978, *Nat*, 275, 372
 Bowler B. P. et al., 2010, *ApJ*, 709, 396
 Burleigh M. R., Clarke F. J., Hodgkin S. T., 2002, *MNRAS*, 331, L41
 Butler R. P., Tinney C. G., Marcy G. W., Jones H. R. A., Penny A. J., Apps K., 2001, *ApJ*, 555, 410
 Butler R. P. et al., 2006, *ApJ*, 646, 505
 Casewell S. L., Dobbie P. D., Napiwotzki R., Burleigh M. R., Barstow M. A., Jameson R. F., 2009, *MNRAS*, 395, 1795
 Chauvin G., Lagrange A. M., Udry S., Fusco T., Galland F., Naef D., Beuzit J. L., Mayor M., 2006, *A&A*, 456, 1165
 Dekker H., D’Odorico S., Kaufer A., Delabre B., Kotzłowski H., 2000, *Proc. SPIE*, 4008, 534
 Desidera S., Barbieri M., 2007, *A&A*, 462, 345
 Drilling J. S., Landolt A. U., 2000, in Cox A. N., ed., *Allen’s Astrophysical Quantities*. Springer, New York
 Farihi J., Barstow M. A., Redfield S., Dufour P., Hambly N. C., 2010, *MNRAS*, 404, 2123

Fontaine G., Brassard P., Bergeron P., 2001, *PASP*, 113, 409
 Gezari D. Y., Pitts P. S., Schmitz M., 2009, *Catalog of Infrared Observations*, 5th edn. CDS, Strasbourg
 Heppenheimer T. A., 1974, *Icarus*, 22, 436
 Holberg J. B., 2009, *J. Phys. Conf. Ser.*, 172, 012022
 Holberg J. B., Bergeron P., 2006, *AJ*, 132, 1221
 Holberg J. B., Sion E. M., Oswalt T., McCook G. P., Foran S., Subasavage J. P., 2008, *AJ*, 135, 1225
 Holden F., 1966, *Publ. Obser. Univ. Michigan*, 9, 185
 Holman M. J., Wiegert P. A., 1999, *ApJ*, 117, 621
 Hurley J. R., Pols O. R., Tout C. A., 2000, *MNRAS*, 315, 543
 Jeans J. H., 1924, *MNRAS*, 85, 2
 Jenkins J. S. et al., 2011, *A&A*, 531, A8
 Jessup M. K., 1955, *Publ. Obser. Univ. Michigan*, 11, 1
 Johnson J. A., Butler R. P., Marcy G. W., Fischer D. A., Vogt S. S., Wright J. T., Peek K. M. G., 2007, *ApJ*, 670, 833
 Kalirai J. S., Hansen B. M. S., Kelson D. D., Reitzel D. B., Rich R. M., Richer H. B., 2008, *ApJ*, 676, 594
 Koester D., 2010, *Mem. Soc. Astron. Ital.*, 81, 921
 Koester D., Rollenhagen K., Napiwotzki R., Voss B., Christlieb N., Homeier D., Reimers D., 2005, *A&A*, 432, 1025
 Koester D., Voss B., Napiwotzki R., Christlieb N., Homeier D., Lisker T., Reimers D., Heber U., 2009, *A&A*, 505, 441.
 Liebert J., Bergeron P., Holberg J. B., 2005, *ApJS*, 156, 47
 Lovis C., Mayor M., 2007, *A&A*, 472, 657
 Martin D. C. et al., 2005, *ApJ*, 619, L1
 Mason B. D., Wycoff G. L., Hartkopf W. I., Douglass G. G., Worley C. E., 2001, *AJ*, 122, 3466
 McCook G. P., Sion E. M., 1999, *ApJS*, 121, 1
 McCook G. P., Sion E. M., 2008, *Catalog of Spectroscopically Identified White Dwarfs*. CDS, Strasbourg
 Morrissey P. et al., 2007, *ApJS*, 173, 682
 Mugrauer M., Neuhäuser R., Mazeh T., 2007, *A&A*, 469, 755
 Napiwotzki R. et al., 2003, *The Messenger*, 112, 25
 Nordhaus J., Spiegel D. S., Ibgui L., Goodman J., Burrows A., 2010, *MNRAS*, 408, 631
 O’Dwyer I. J., Chu Y. H., Gruendl R. A., Guerrero M. A., Webbink R. F., 2003, *AJ*, 125, 2239
 Perryman M. A. C. et al., 1997, *A&A*, 323, L49
 Raghavan D., Henry T. J., Mason B. D., Subasavage J. P., Jao W. C., Beaulieu T. D., Hambly N. C., 2006, *ApJ*, 646, 523
 Siess L., Livio M., 1999a, *MNRAS*, 304, 925
 Siess L., Livio M., 1999b, *MNRAS*, 308, 1133
 Sion E. M., Holberg J. B., Oswalt T. D., McCook G. P., Wasatonic R., 2009, *AJ*, 138, 1681
 Su K. Y. L. et al., 2006, *ApJ*, 653, 675
 Takeda G., Ford E. B., Sills A., Rasio F. A., Fischer D. A., Valenti J. A., 2007, *ApJS*, 168, 297
 Tremblay P.-E., Bergeron P., 2009, *ApJ*, 696, 1755
 Trilling D. E. et al., 2008, *ApJ*, 674, 1086
 van Leeuwen F., 2007, *A&A*, 474, 653
 Voges W. et al., 2000, *The ROSAT All-Sky Survey Faint Source Catalog*. CDS, Strasbourg
 Williams K. A., Bolte M., Koester D., 2009, *ApJ*, 693, 355
 Wilson R. E., 1953, *The General Catalog of Stellar Radial Velocities*. Carnegie Institution of Washington, Washington
 Zuckerman B., Koester D., Reid I. N., Hünsch M., 2003, *ApJ*, 596, 477
 Zuckerman B., Melis C., Klein B., Koester D., Jura M., 2010, *ApJ*, 722, 725

This paper has been typeset from a $\text{\TeX}/\text{\LaTeX}$ file prepared by the author.